Spectrochimica Acta Part A: Molecular and Biomolecular Spectroscopy 183 (2017) 356–361

Contents lists available at ScienceDirect

Spectrochimica Acta Part A: Molecular and Biomolecular Spectroscopy

journal homepage: www.elsevier.com/locate/saa

A novel pyridyl triphenylamine–BODIPY aldoxime: Naked-eye visible and fluorometric chemodosimeter for hypochlorite

Xiu-xiu Xu, Ying Qian *

School of Chemistry and Chemical Engineering, Southeast University, Nanjing, China

ARTICLE INFO

Article history:
Received 19 December 2016
Received in revised form 18 March 2017
Accepted 18 April 2017
Available online 20 April 2017

Keywords:
Aldoxime
Triphenylamine–BODIPY
Hypochlorite detection
C═N isomerization
Naked-eye visible

ABSTRACT

An aldoxime containing fluorescent probe based on vinylpydine-appended triphenylamine–BODIPY has been designed and used for hypochlorite detection. OX-PPA-BODIPY was developed by introducing an aldoxime group into the 2-position of BODIPY, which can be used for the detection of hypochlorite with a sharp color change from pink to green. The attachment of 4-vinylpyridine moiety to triphenylamine–BODIPY constructs a fluorogen with desirable conjugated system. The probe, which displays extremely weak fluorescence owing to the C═N isomerization mechanism at 2-position of BODIPY, responds to HClO/ClO^- through a dramatic enhancement of its fluorescence intensity. This new probe, a naked-eye visible and fluorometric chemodosimeter, exhibits high selectivity and sensitivity toward hypochlorite over other reactive oxygen species (ROS) and anions. The detection is accompanied by a 20-fold increase in fluorescent intensity (Φ_F from 0.02 to 0.43). The detection limit of the probe for hypochlorite is 7.37×10^{-7} M. Moreover, OX-PPA-BODIPY can be used to detect hypochlorite in real water samples.

1. Introduction

Hypochlorous acid (HClO)/hypochlorite (ClO^-) is known to be a kind of biologically important reactive oxygen species (ROS) [1]. In living organisms, hypochlorous acid is produced predominantly from hydrogen peroxide and chloride ions in a chemical reaction catalyzed by the heme enzyme myeloperoxidase (MPO), which plays a pivotal role in the immune defense against microorganisms and in inflammation [2–5]. However, excessive amounts of hypochlorous acid/hypochlorite in the physiological and pathological processes can lead to various diseases, such as atherosclerosis, osteoarthritis, rheumatoid arthritis and even cancers [6–10]. Thus, monitoring HClO/ClO^- in living organisms is highly demanded for the research in biology and medicine.

Fluorescent probes have been evaluated as powerful tools to detect biological agents in recent years, due to their high sensitivity and selectivity, real-time detection and easiness of manipulating [11–13]. In recent years, a number of fluorescent probes for HClO/ClO^- based on unique reaction mechanisms have been developed, including oxidation of p-methoxyphenol to benzoquinone [14], selenide to selenoxide [15–17], oxime to aldehyde [18], and others [19]. Most of them are based on different fluorophores that included rhodamine [20], boradiazaindacene (BODIPY) [21], fluorescein [22], naphthalimide [23] and so on [24]. Chen et al. [25] developed a highly selective turn-on fluorescent probe for hypochlorous acid based on hypochlorous acid-induced oxidative intramolecular cyclization of boron dipyrromethene-hydrazone. Cheng [26] and his coworkers have demonstrated a highly sensitive and selective hypochlorite fluorescent probe based on oxidation of hydrazine via free radical mechanism. Mulay's group [27] constructed two closely related phenyl selenyl based boron-dipyrromethene turn-on fluorescent probes for the detection of hypochlorous acid (HClO). Sun [28] and his group developed a probe for hypochlorous acid based on the cleavage of carbon-carbon double bonds. Liu [29] synthesized a highly sensitive and selective hypochlorite fluorescent probe based on oxidation of hydrazine via free radical mechanism. Recently, BODIPY dyes has attracted more and more attention because of its exceptional photophysical properties such as long emission wavelengths, high molar absorption coefficients and fluorescence quantum yield [30–33]. In addition, BODIPY, a group of luminogenic molecules, is easy to modify to obtain desirable performance. According to the previous work, the reports on the probe for HClO/ClO^- based on BODIPY are still limited. A number of BODIPY-based HClO/ClO^- probes have been reported, however, emission band of these probes majorly falled into the region of 500–520 nm. Therefore, the development of fluorescent probes for HClO/ClO^- based on BODIPY is in urgent demand.

In our work, a naked-eye visible and fluorometric chemodosimeter based on the HClO/ClO^--promoted oxidation of aldoxime for hypochlorite was designed by combining pyridyl triphenylamine and BODIPY. Based on the deoximation reaction some fluorescent probes were designed. Compared with the previous reported sensors [34–36], the structure of dye moiety is novel and used for the first time to sense hypochlorite. As we know, triphenylamine-BODIPY derivatives with their emissions are tunable from green to red exhibit highly efficient and stable photophysical properties [37]. Therefore, triphenylamine–BODIPY

* Corresponding author.
E-mail address: yingqian@seu.edu.cn (Y. Qian).

http://dx.doi.org/10.1016/j.saa.2017.04.043
1386-1425/

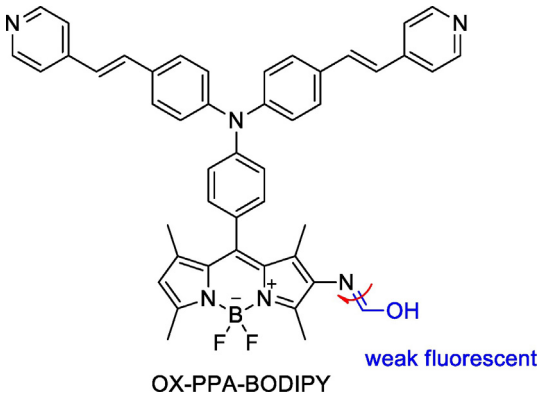

Scheme 1. Chemical structures of pyridyl triphenylamine–BODIPY aldoxime.

was adopted as fluorogenic moiety. The attachment of 4-vinylpyridine moiety to triphenylamine–BODIPY can successfully build a new fluorogen and extend the conjugation system. In this probe, an aldoxime group was employed as hypochlorite-responsive moiety. As shown in Scheme 1, due to C═N isomerization, the probe is weak fluorescent. OX-PPA-BODIPY could react rapidly with HClO/ClO^-, while HClO/ClO^- mediated removal of the aldoxime group restores the fluorescence of the BODIPY fluorogenic moiety.

2. Experiment

2.1. Chemicals and Instruments

Chemical structures were confirmed by NMR analysis and mass spectrometry. ^{1}H NMR and ^{13}C NMR spectra were recorded on a Bruker 300 MHz spectrometer and a Bruker 300 MHz spectrometer in $CDCl_3$ with tetramethylsilane (TMS) as internal standard. Chemical shifts are given in parts per million (ppm). Mass spectra were recorded on Agilent Technologies 6530 Accurate-Mass Q-TOF LC/MS. UV–visible absorption spectra were determined on a Shimadzu UV-3600 spectrophotometer. Fluorescence spectra were measured on a HORIBA FL-4 Max spectrometer. 1 × 1 × 3 cm quartz cuvettes were used for absorption and emission spectral titration.

All reagents used were purchased and used without further purification. All solvents used in spectroscopic measurements were of analytical grade. Reactions were monitored by thin layer chromatography using Merck TLC Silica gel 60 F254. Silica gel column chromatography was performed over Merck Silica gel 60.

2.2. Synthesis

The synthetic routes are presented in Scheme 2. 2,4-dimethyl-pyrrole, *N*,*N*-di (4-iodophenyl) aminobenzaldehyde, and other important intermediates were synthesized according to literature procedures [38–39]. All chemical structures were confirmed by ^{1}H NMR, ^{13}C NMR and mass spectrometry.

8-{4-{*N*,*N*-bis{4-[2-(4-pyridyl)ethenyl]phenyl}amino}phenyl}-1,3,5,7-tetramethyl-4,4′-difluoro-4-bora-3a,4a-diaza-s-indacene(PPA-BODIPY). A mixture of IPA-BODIPY (0.50 g, 0.67 mmol), 4-vinylpyridine (0.17 g, 1.62 mmol), $Pd(OAc)_2$ (4.53 mg, 0.02 mmol), K_3PO_4 (0.21 g, 1.01 mmol) and Tri(o-tolyl)phosphine (0.02 g, 0.07 mmol) in DMF (6 mL)was stirred for 24 h at the temperature of 130 °C in nitrogen atmosphere. Then, the reaction mixture was brought to room temperature, washed with water and extracted by filtration method. The residue was purified by column chromatography on silica gel to obtain the pure product PPA-BODIPY as an orange powder in 75.8% yield. ^{1}H NMR (300 MHz, $CDCl_3$) δ: 8.57 (d, *J* = 3.00 Hz, 4H), 7.48 (d, *J* = 9.00 Hz, 4H), 7.35 (d, *J* = 6.00 Hz, 4H), 7.27 (m, 4H),7.19 (d, *J* = 9.00 Hz, 2H), 7.13 (d, *J* = 9.00 Hz, 4H), 6.94 (d, *J* = 15.00 Hz, 2H),

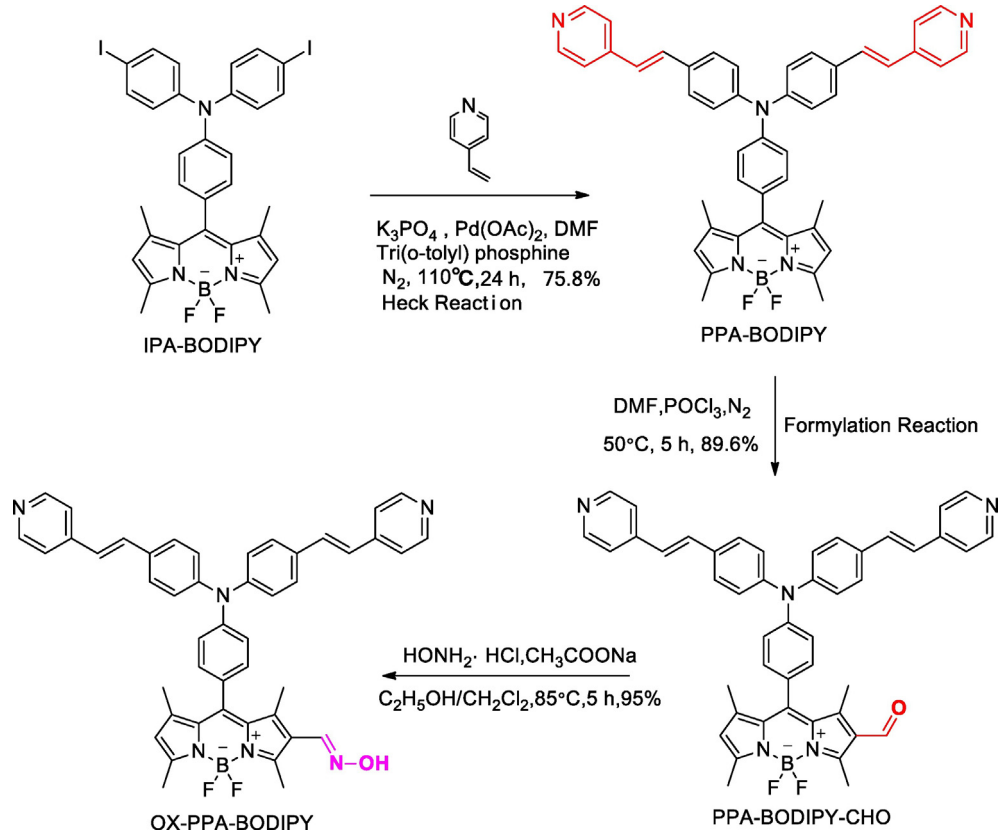

Scheme 2. Synthesis of pyridyl triphenylamine-BODIPY derivative.

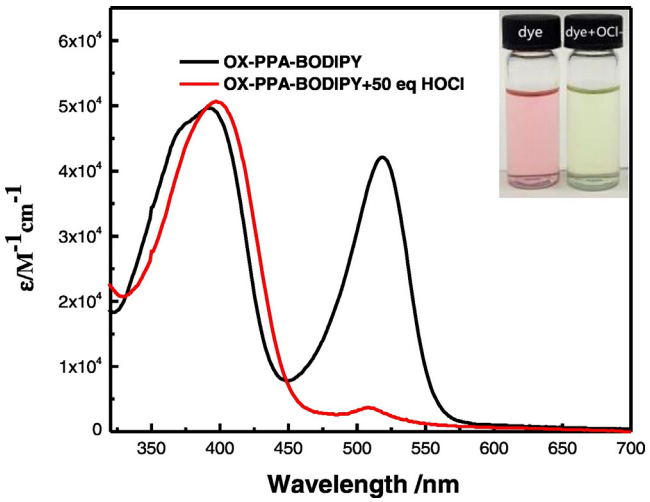

Fig. 1. Absorption spectra of OX-PPA-BODIPY (10^{-5} M) and OX-PPA-BODIPY + HOCl (5×10^{-4} M, 50 equiv.) in PBS buffer (pH = 7.4) and THF mixed solvent systems (1/1, v/v). Inset: the colorimetric detection of HOCl.

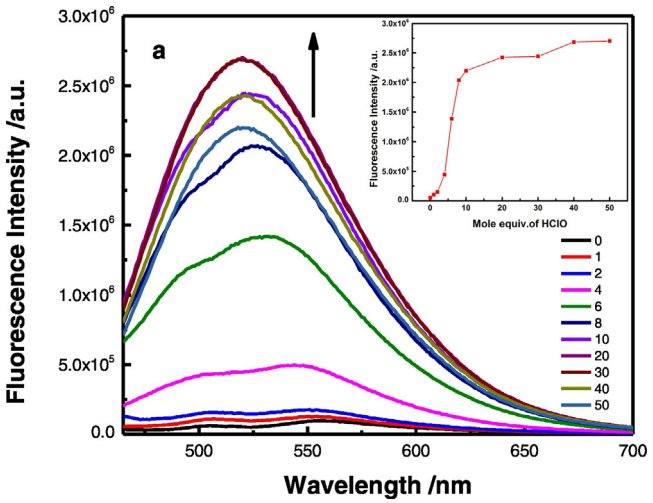

Fig. 3. Fluorescence spectra of probe OX-PPA-BODIPY (10 μM) with increasing amount of NaOCl in PBS buffer (pH = 7.4) and THF (1/1, v/v) solution. The excitation wavelength was 450 nm.

6.02 (s, 2H), 2.56 (s, 6H), 1.60 (s, 6H). ^{13}C NMR (300 MHz, $CDCl_3$) δ: 155.52, 149.96, 147.59, 147.33, 144.89, 142.75, 141.35, 132.42, 131.40, 129.88, 129.33, 128.28, 124.91, 124.81, 124.24, 121.30, 120.73, 14.55. HRMS-MALDI-TOF calcd for $C_{45}H_{38}BF_2N_5$ $[M + H]^+$ = 698.3261 found: 698.3228.

8-{4-{*N*,*N*-bis{4-[2-(4-pyridyl)ethenyl]phenyl}amino}phenyl}-2-formyl-1,3,5,7-tetramethyl-4,4′-difluoro-4-bora-3a,4a-diaza-s-indacene(PPA-BODIPY-CHO). DMF (6 mL) was stirred in ice bath and $POCl_3$ (6 mL) was added dropwise. After the solution was warmed to room temperature, it was stirred for additional 30 min. PPA-BODIPY (0.50 g, 0.60 mmol) in dichloroethane (30 mL) was added to this reaction mixture. The temperature was raised to 60 °C, and the mixture was stirred for an additional 3 h. The reaction mixture was cooled to room temperature and slowly poured in saturated aqueous $NaHCO_3$ (150 mL) under ice-cold condition, which was extracted CH_2Cl_2. After the evaporation of CH_2Cl_2, the residue was purified by silica gel column chromatography to get the pure product PPA-BODIPY-CHO as a deep red powder in 89.6% yield. ^{1}H NMR (300 MHz, $CDCl_3$) δ: 10.07 (s, 1H), 8.59 (d, *J* = 6.00 Hz, 4H), 7.52 (d, *J* = 6.00 Hz, 4H), 7.37 (d, *J* = 6.00 Hz, 4H), 7.33–7.27 (m, 4H), 7.22–7.14 (m, 4H), 6.98 (d, *J* = 15.00 Hz, 2H), 6.22 (s, 1H), 2.84 (s, 3H), 2.65 (s, 3H), 1.81 (s, 3H), 1.69 (s, 3H). ^{13}C NMR (300 MHz, $CDCl_3$) δ: 185.85, 150.02, 147.14, 144.80, 132.31, 131.73, 129.11, 128.34, 125.15, 124.84, 124.48, 120.73, 53.38, 29.66, 15.10, 12.84, 11.91. HRMS-MALDI-TOF calcd for $C_{46}H_{38}BF_2N_5O$ $[M + H]^+$ = 726.3215 found: 726.3267.

8-{4-{*N*,*N*-bis{4-[2-(4-pyridyl)ethenyl]phenyl}amino}phenyl}-2-(hydroxyimino)methyl-1,3,5,7-tetramethyl-4,4′-difluoro-4-bora-3a,4a-diaza-s-indacene(OX-PPA-BODIPY). PPA-BODIPY-CHO(0.15 g, 0.210 mmol)was dissolved in methylene chloride and ethanol mixed solvent(30 mL),and excess hydroxylammonium chloride(0.04 g, 0.630 mmol) was added, then sodium acetate(0.08 g, 0.944 mmol)was added as catalyst. The mixture was stirred for 5 h at 85 °C. After the evaporation of CH_2Cl_2 and C_2H_5OH, the residue was purified by silica gel column chromatography to afford the final product OX-PPA-BODIPY as an orange red powder in 95% yield. ^{1}H NMR (300 MHz, $CDCl_3$) δ: 8.57 (d,6.00 Hz,4H), 8.15 (s,1H), 7.49 (d,9.00 Hz,4H), 7.36 (d,6.00 Hz,4H), 7.30–7.26 (m,5H), 7.19 (d,9.00 Hz,2H), 7.13 (d,6.00 Hz,4H), 6.95 (d,15.00 Hz, 2H), 6.08 (s,1H), 2.65 (d,12.00 Hz, 6H), 1.66 (d,27.00 Hz,6H). ^{13}C NMR (300 MHz, $CDCl_3$) δ: 160.69,157.44, 152.72,150.80,150.25,147.75, 147.69,147.25,144.97,142.53,136.23, 135.40,134.51,133.82,132.48,132.33,131.30,128.03,127.73,127.33,125.3-7,125.09,80.43,80.00,79.58,32.66,17.80,16.91,15.64. HRMS-MALDI-TOF calcd for $C_{46}H_{39}BF_2N_6O$ $[M + H]^+$ = 741.3324 found: 741.3341.

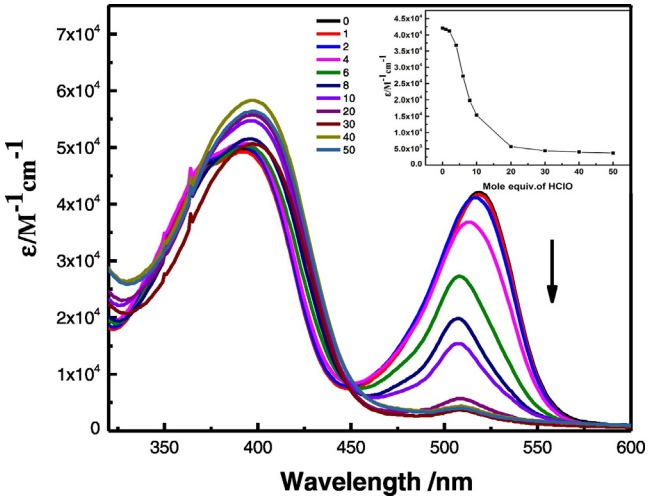

Fig. 2. Absorption spectra of probe OX-PPA-BODIPY (10 μM) with increasing amount of NaOCl in PBS buffer (pH = 7.4) and THF (1/1, v/v) solution.

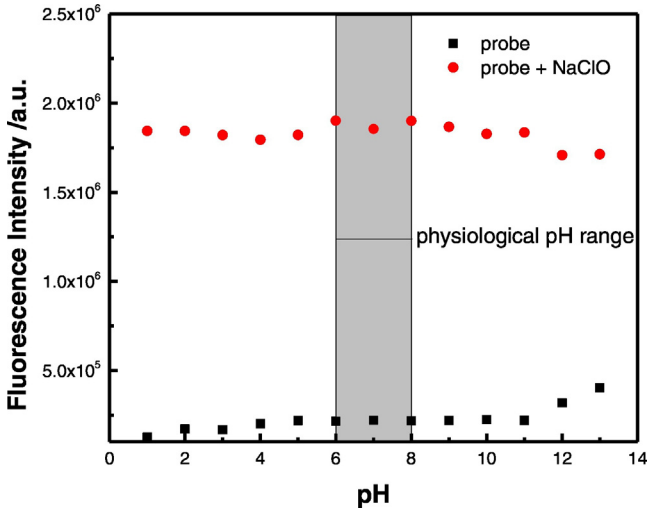

Fig. 4. Fluorescence intensity of OX-PPA-BODIPY (10^{-5} M) in the absence (■) or presence (●) of OCl^- (10×10^{-5} M) as a function of pH. Excitation wavelength was 450 nm.

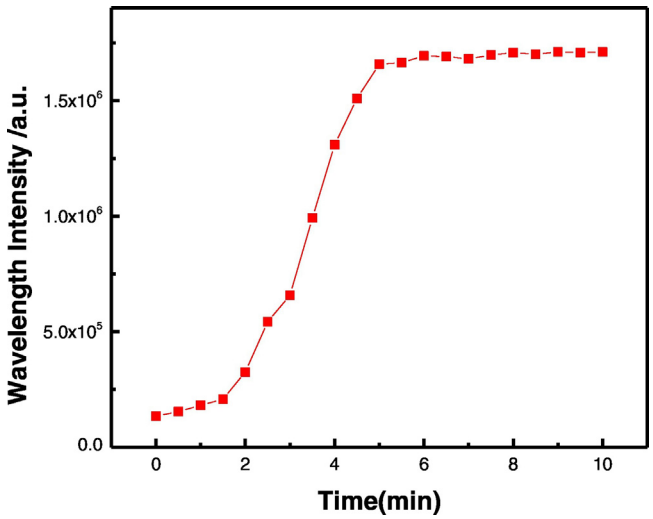

Fig. 5. Time dependent fluorescence intensity changes of probe OX-PPA-BODIPY (10^{-5} M) with 10 equiv. NaClO in a mixture of PBS buffer (pH = 7.4) and THF (1/1, v/v, λ_{ex} = 450 nm).

3. Results and Discussion

3.1. Design and Synthesis of Pyridyl Triphenylamine-BODIPY Aldoxime

The synthetic routes of the probe OX-PPA-BODIPY are shown in Scheme 2. The detailed synthetic procedures and data of the structure characterization are described in the Experimental section and Supporting information. Our strategy is based on the following design principles: Firstly, triphenylamine–BODIPY was adopted as fluorogenic moiety. Secondly, the modifier of pyridine linked to the triphenylamine–BODIPY core with C═C double bond will extend the conjugation and lead to a redshifted emission. Finally, the introduction of an aldoxime unit at the 2-position of BODIPY was used as "off - on" reactor. PPA-BODIPY was synthesized through Palladium-catalyzed Heck reaction of TPA-BODIPY with 4-vinylpyridine with good yield (75.8%). Through such synthetic routes, 4-vinylpyridine substituents are linked to BODIPY core on 8-position through a vinyl bridge. PPA-BODIPY-CHO was obtained by formylation reaction of PPA-BODIPY. Afterwards PPA-BODIPY-CHO was allowed to react with $HONH_2 \cdot HCl$ to produce the final product OX-PPA-BODIPY. The compounds were confirmed by magnetic resonance (^{1}H NMR and ^{13}C NMR) and high resolution mass spectrometry (HRMS-MALDI-TOF). The structural characterization data of the product by spectroscopic methods are given in the Experimental Section. The purity of the resultant products and intermediates has been confirmed by ^{1}H NMR, ^{13}C NMR, and high-resolution mass (MALDI-TOF) spectroscopic techniques (see Figs. S1–S5, Supporting information).

3.2. Naked-eye Visible and Fluorometric Chemodosimeter for Hypochlorous Acid

The spectral properties of the probe toward the addition of ClO^- were examined in PBS buffer (pH = 7.4) and THF mixed solvent systems (1/1, v/v) was shown in Fig. 1. According to Fig.1, two major absorption bands of OX-PPA-BODIPY located at 393 nm and 520 nm are observed. The former is ascribed to the localized π-π* transition of aromatic moieties in the molecular level, while the latter attributed to the BODIPY core with attachment of aldoxime. Meanwhile, upon addition of ClO^- to the solution of OX-PPA-BODIPY, the absorption peak located at 520 nm decreased dramatically (Fig. 2). Accordingly, the addition of ClO^- to the probe produces a colorimetric change from pink to green, which can be detected by the naked eye (Fig. 1).

The plot of the fluorescence intensity of OX-PPA-BODIPY against the increase in ClO^- concentration is displayed in Fig. 3. As shown, OX-PPA-BODIPY in solution is weak emissive (Φ_F = 0.02) possibly due to a non-radiative deactivation through rapid isomerization of the C═N—OH group. The emission spectra of PPA-BODIPY displays two emission peaks located at 508 nm and 555 nm. The detection of OX-PPA-BODIPY toward ClO^- were studied by addition of different equivalent of ClO^- solution (0–50 equivalent) to a solution of OX-PPA-BODIPY in PBS buffer (pH = 7.4) with 50% water (Fig. 1). From Fig. 3, the intensity of the emission

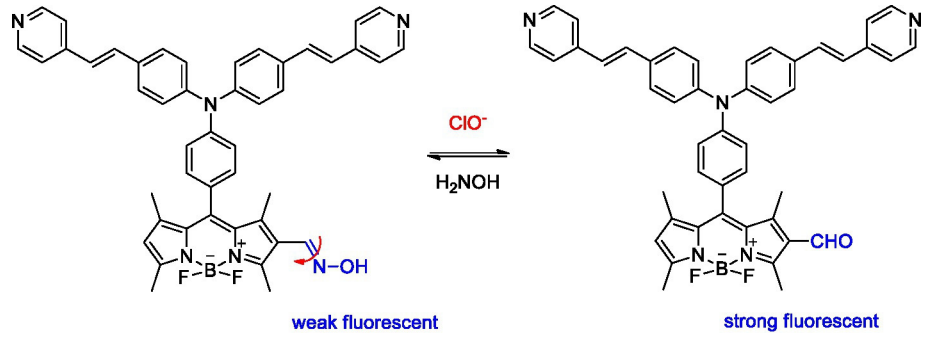

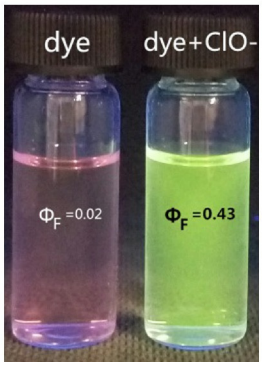

Scheme 3. OCl^- promoted oxidative deoximation reaction of OX-PPA-BODIPY.

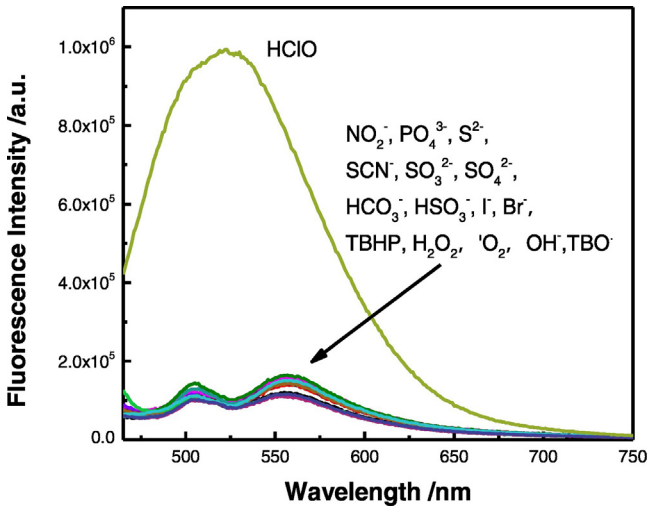

Fig. 6. Fluorescence responses of OX-PPA-BODIPY (10^{-5} M) to NaClO (10 equiv.) and other ROS and different anions at 520 nm. Conditions: PBS buffer (pH = 7.4) and THF (1/1, v/v). λ_{em} = 450 nm.

peaks at 508 nm and 550 nm both increased, gradually merging into a peak at 520 nm, which also resulted in a visual fluorescence change (from pink to green) under illumination with a 365 nm UV lamp. When the amount of ClO^- added reached 50 equivalents with respect to the probe, these changes were found to reach a plateau, with a 20-fold fluorescence enhancement accompanied. Fluorescence titration was carried out in PBS-buffered solution (pH = 7.4) to determine the detection limit, which was then calculated with the equation: detection limit = 3σ/k [40], where σ is the standard deviation of blank measurements, and k is the slope between intensity and sample concentration. Thus, the detection limit was determined to be 7.37×10^{-7} M.

In addition, a pH-dependence experiment of OX-PPA-BODIPY was conducted to investigate a suitable pH range for ClO^- sensing. The pH titration curve (Fig. 4) also reveals that the fluorescence intensity of OX-PPA-BODIPY and the corresponding product toward ClO^- maintain almost constant values at pH 1–13, demonstrating that OX-PPA-BODIPY can work in the biological pH range without influence.

More, Time-dependent modulations in the fluorescence spectra of the probe were monitored in the presence of 10 equiv. of ClO^- (Fig. 5). The kinetic study showed that the reaction was completed within 5 min for ClO^-, indicating that the probe reacts rapidly with ClO^- under the experimental conditions. The addition of ClO^- (aq.) to a solution containing OX-PPA-BODIPY results in an immediate, strong increase in the fluorescence intensity (Fig. 3). During the titration of ClO^- with OX-PPA-BODIPY, a new emission band appeared at 520 nm. The emission intensity reached its maximum after the addition of one equivalent of ClO^-. The quantum yield of the oxidized form was 0.43, which is 21-fold greater than that of OX-PPA-BODIPY (0.02).

The reaction mechanism of the present system was investigated. It is assumed that the color change and fluorescence increasing could be attributed to aldoxime oxidation to aldehydes in the presence of ClO^- (Scheme 3). As we all known, the removal of a C═N bond in a fluorogenic molecule via the reaction of an oxime and ClO^- restores the strong fluorescence. It is speculated that the mechanism is based on a specific reaction promoted by hypochlorite. The HRMS spectra of the reaction mixture of OX-PPA-BODIPY with OCl^- (Fig. S6) verified the aldoxime oxidation to aldehyde, which showed peaks at 748.5490/764.5820 (for $[PPA\text{-}BODIPY\text{-}CHO + Na]^+$ / $[PPA\text{-}BODIPY\text{-}CHO + K]^+$).

3.3. Response of OX-PPA-BODIPY to Different Anions and ROS

Selectivity is the most important requirement for all kinds of detection methods. The turn-on response of OX-PPA-BODIPY to other reactive oxygen species (ROS) such as TBHP, H_2O_2, O_2, ·OH, TBO· and anions including NO_2^-, PO_4^{3-}, S^{2-}, SCN^-, SO_3^{2-}, SO_4^{2-}, HCO_3^-, HSO_3^-, I^-, Br^- was also tested. In the test system, 10 equiv. ClO^- as well as other ROS and different anions were added respectively to a 10^{-5} M solution of OX-PPA-BODIPY. Only ClO^- induced robust fluorescence intensity enhancement, other analytes show negligible changes in absorbance spectra under the same conditions. As shown in Fig. 6, only ClO^- caused a robust fluorescence intensity enhancement while the others exhibited almost no change in fluorescence behaviour. A significant feature of the probe was its high selectivity toward ClO^- over other competitive ROS and different anions (Fig. 7). The result indicated that OX-PPA-BODIPY showed high sensitivity toward hypochlorite with low interference. The detailed photophysical properties of OX-PPA-BODIPY and OX-PPA-BODIPY + ClO^- in a mixture of PBS buffer (pH = 7.4) and THF (1/1, v/v) were summarized in Table 1.

4. Conclusions

In summary, a fluorescence probe OX-PPA-BODIPY based on triphenylamine-BODIPY platform that can selectively detect HClO/ClO^- over other ROS species and anions in aqueous media. The probe exhibited an obvious HClO/ClO^- induced a large fluorescence enhancement in the emission spectra resulting in a change of solution color from pink to green with fast response and selectivity. Furthermore, OX-PPA-BODIPY was almost nonfluorescent (turn-off) and the fluorescence emission of the probe can be turned on upon addition of HClO/ClO^-, which resulted in an increase of the emission intensity up to 20-fold with fluorescence quantum yield of 0.43. The addition of HClO/ClO^- to the probe solution developed an instantaneous color and fluorescence change. Which was easily detectable by the naked eyes under light and UV irradiation. The detection limit of OX-PPA-BODIPY was measured to be 7.37×10^{-7} M. This probe is expected to be a useful tool in various biological and pathological processes.

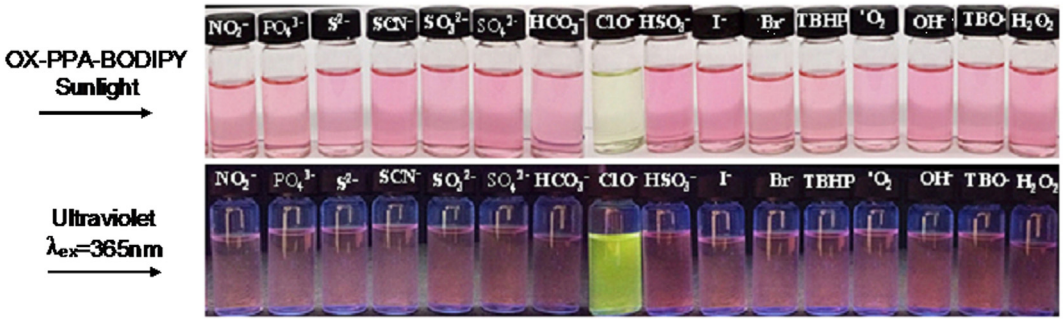

Fig. 7. The corresponding photographs of dosimeter OX-PPA-BODIPY after the addition NaClO (10 equiv.) and other ROS and different anions in aqueous media. Conditions: PBS buffer (pH = 7.4) and THF (1/1, v/v).

Table 1
Photophysical properties of OX-PPA-BODIPY and OX-PPA-BODIPY + NaOCl in a mixture of PBS buffer (pH = 7.4) and THF (1/1, v/v).

Compounds	λ_{ab} (nm)	ε_{max} (10^4 $cm^{-1} * M^{-1}$)	λ_{em} (nm)	Φ_F
OX-PPA-BODIPY	393	4.94	550	0.02
	520	4.22		
OX-PPA-BODIPY + ClO^-	399	5.09	520	0.43
	510	0.37		

λ_{ab} UV absorption; λ_{em} fluorescence emission maximum; ε_{max} maximum molar extinction coefficient; Φ_F fluorescence quantum yield.

Acknowledgements

This work was financially supported by the Fundamental Research Funds (61178057) for the National Natural Science Foundation of China (No. 61178057).

Appendix A. Supplementary Data

Supplementary data to this article can be found online at http://dx.doi.org/10.1016/j.saa.2017.04.043.

References

[1] H. Zhu, J. Fan, J. Wang, et al., An "enhanced-PET" based fluorescent probe with ultrasensitivity for imaging basal and elesclomol-induced HClO in cancer cells, J. Am. Chem. Soc. 136 (2014) 12820–12823.
[2] Y. Yue, F. Huo, F. Yin, et al., Correction: an ICT based ultraselective and sensitive fluorescent probe for detection of HClO in living cells, RSC Adv. 5 (2015) 77670–77672.
[3] K. Xiong, F. Huo, C. Yin, et al., A highly selective fluorescent bioimaging probe for hypochlorite based on 1,8-naphthalimide derivative, Sensors Actuators B Chem. 221 (2015) 1508–1514.
[4] W.C. Chen, P. Venkatesan, S.P. Wu, A turn-on fluorescent probe for hypochlorous acid based on HOCl-promoted removal of the C=N bond in BODIPY-hydrazone, New J. Chem. 39 (2015) 6892–6898.
[5] Y. Shen, X. Zhang, X. Huang, et al., A simple and reversible fluorescent probe based on NBD for rapid detection of hypochlorite and its application for bioimaging, RSC Adv. 5 (2015) 79519–79524.
[6] J. Li, F. Huo, C. Yin, A selective colorimetric and fluorescent probe for the detection of ClO^- and its application in bioimaging, RSC Adv. 4 (2014) 6669–6684.
[7] B. Wang, P. Li, F. Yu, et al., A reversible fluorescence probe based on Se-BODIPY for the redox cycle between HClO oxidative stress and H_2S repair in living cells, Chem. Commun. 49 (2013) 1014–1016.
[8] L. Wang, L. Long, L. Zhou, et al., A ratiometric fluorescent probe for highly selective and sensitive detection of hypochlorite based on the oxidation of N-alkylpyridinium, RSC Adv. 4 (2014) 59535–59540.
[9] G. Wu, F. Zeng, S. Wu, A water-soluble and specific BODIPY-based fluorescent probe for hypochlorite detection and cell imaging, Anal. Methods 5 (2013) 5589–5596.
[10] X. Zeng, L.J. Liang, C. Liu, et al., Highly selective and sensitive photoinduced electron transfer (PET) based HOCl fluorescent probe in water and its endogenous imaging in living cells, Chem. Commun. 52 (2016) 7982–7985.
[11] B.X. Shen, Y. Qian, A novel triphenylamine-BODIPY dendrons: click synthesis, near-infrared emission and multi-channel chemodosimeter for Hg^{2+} and Fe^{3+}, J. Mater. Chem. B 4 (2016) 7549–7559.
[12] B.X. Shen, Y. Qian, Click synthesis, Hg^{2+}, sensor and intramolecular fluorescence resonance energy transfer in novel BODIPY dendrons, Sensors Actuators B Chem. 239 (2016) 226–234.
[13] B.X. Shen, Y. Qian, A novel fluorescent dye: synthesis, fluorescence resonance energy transfer and cell imaging, Chin. J. Org. Chem. 36 (2016) 774–781.
[14] K. Cui, D. Zhang, G. Zhang, et al., A highly selective naked-eye probe for hypochlorite with the p-methoxyphenol-substituted aniline compound, Tetrahedron Lett. 51 (2010) 6052–6055.
[15] H. Ren, Y. Wu, N. Ma, et al., Side-chain selenium-containing amphiphilic block copolymers: redox-controlled self-assembly and disassembly, Soft Matter 8 (2011) 1460–1466.
[16] Z. Lou, P. Li, Q. Pan, et al., A reversible fluorescent probe for detecting hypochloric acid in living cells and animals: utilizing a novel strategy for effectively modulating the fluorescence of selenide and selenoxide, Chem. Commun. 49 (2013) 2445–2447.
[17] J.M. Khurana, B.M. Kandpal, Y.K. Chauhan, Rapid oxidation of selenides, selenoxides, tellurides, and telluroxides with aqueous sodium hypochlorite, Phosphorus Sulfur Silicon Relat. Elem. 178 (2003) 1369–1375.
[18] J. Shi, Q. Li, X. Zhang, et al., Simple triphenylamine-based luminophore as a hypochlorite chemosensor, Sensors Actuators B Chem. 145 (2010) 583–587.
[19] S.Y. Yu, C.Y. Hsu, W.C. Chen, et al., A hypochlorous acid turn-on fluorescent probe based on HOCl-promoted oxime oxidation and its application in cell imaging, Sensors Actuators B Chem. 196 (2014) 203–207.
[20] (a) S. Kenmoku, Y. Urano, H. Kojima, et al., Development of a highly specific rhodamine-based fluorescence probe for hypochlorous acid and its application to real-time imaging of phagocytosis, J. Am. Chem. Soc. 129 (2007) 7313–7318;
(b) L. Yuan, W. Lin, Y. Xie, et al., Fluorescent detection of hypochlorous acid from turn-on to FRET-based ratiometry by a HOCl-mediated cyclization reaction, Chem. Eur. J. 18 (2012) 2700–2706.
[21] H. Xiao, K. Xin, H. Dou, et al., A fast-responsive mitochondria-targeted fluorescent probe detecting endogenous hypochlorite in living RAW 264.7 cells and nude mouse, Chem. Commun. 51 (2015) 1442–1445.
[22] W. Yin, H. Zhu, R. Wang, A sensitive and selective fluorescence probe based fluorescein for detection of hypochlorous acid and its application for biological imaging, Dyes Pigments 107 (2014) 127–132.
[23] J. Li, P. Li, F.J. Huo, et al., Ratiometric fluorescent probes for ClO^-, and in vivo applications, Dyes Pigments 130 (2016) 209–215.
[24] S. Wybraniec, K. Starzak, Z. Pietrzkowski, Chlorination of betacyanins in several hypochlorous acid systems, J. Agric. Food Chem. 64 (2016) 2865–2874.
[25] N. Boens, V. Leen, W. Dehaen, Fluorescent indicators based on BODIPY, Chem. Soc. Rev. 41 (2012) 1130–1172.
[26] T. Cheng, J. Zhao, Z. Wang, et al., A highly sensitive and selective hypochlorite fluorescent probe based on oxidation of hydrazine via free radical mechanism, Dyes Pigments 126 (2016) 218–223.
[27] N. Gupta, S.I. Reja, V. Bhalla, et al., A bodipy based fluorescent probe for evaluating and identifying cancer, normal and apoptotic C6 cells on the basis of changes in intracellular viscosity, J. Mater. Chem. B 4 (2016) 1968–1977.
[28] S. Saha, H. Agarwalla, H. Gupta, et al., New chemodosimetric probe for the specific detection of Hg^{2+} in physiological condition and its utilisation for cell imaging studies, Dalton Trans. 42 (2013) 15097–150105.
[29] W.C. Chen, P. Venkatesan, S.P. Wu, A highly selective turn-on fluorescent probe for hypochlorous acid based on hypochlorous acid-induced oxidative intramolecular cyclization of boron dipyrromethene-hydrazone, Anal. Chim. Acta 882 (2015) 68–75.
[30] J. Kang, F. Huo, Y. Yue, et al., A solvent depend on ratiometric fluorescent probe for hypochlorous acid and its application in living cells, Dyes Pigments 136 (2016) 852–858.
[31] S.V. Mulay, M. Choi, Y.J. Jang, et al., Enhanced fluorescence turn-on imaging of hypochlorous acid in living immune and cancer cells, Chem. Eur. J. 22 (2016) 9642–9648.
[32] (a) L. Zhang, Y. Chen, J. Jiang, Solid state fluorescent functionalized-triphenylamine Bodipy detector for HCl vapor with high stability and absolute fluorescent quantum yield, Dyes Pigments 124 (2016) 110–119;
(b) Y. Yang, Z. Lei, B. Li, et al., Triphenylamine-cored tetramethyl-BODIPY dyes: synthesis, photophysics and lasing properties in organic media, RSC Adv. 3 (2013) 14993–14996;
(c) E. Lager, J. Liu, A. Aguilar-Aguilar, et al., Novel meso-polyarylamine-BODIPY hybrids: synthesis and study of their optical properties, J. Organomet. Chem. 74 (2009) 2053–2058.
[33] M. Sun, H. Yu, H. Zhu, et al., Oxidative cleavage-based near-infrared fluorescent probe for hypochlorous acid detection and myeloperoxidase activity evaluation, Anal. Chem. 86 (2014) 671–677.
[34] S.I. Reja, V. Bhalla, A. Sharma, et al., A highly selective fluorescent probe for hypochlorite and its endogenous imaging in living cells, Chem. Commun. 50 (2015) 11911–11914.
[35] S.K. Lee, M.G. Choi, S.K. Chang, Signaling of chloramine: a fluorescent probe for trichloroisocyanuric acid based on deoximation of a coumarin oxime, Tetrahedron Lett. 55 (2014) 7047–7050.
[36] N. Zhao, Y.H. Wu, R.M. Wang, et al., An iridium(III) complex of oximated 2,2′-bipyridine as a sensitive phosphorescent sensor for hypochlorite, Analyst 136 (2011) 2277–2282.
[37] Q. Li, Y. Qian, Aggregation-induced emission enhancement and cell imaging of a novel (carbazol-N-yl)triphenylamine-BODIPY, New J. Chem. 40 (2016) 7095–7101.
[38] Y. He, M. Lin, Z. Li, et al., Direct synthesis of chiral 1,2,3,4-tetrahydropyrrolo[1,2-a]pyrazines via a catalytic asymmetric intramolecular aza-Friedel-crafts reaction, ChemInform 43 (2012) 4490–4493.
[39] A. Zhong, L. Teng, T. Sun, et al., Triphenylamine-based π-conjugated dendrimers: convenient synthesis, easy solution processability, and good hole-transporting properties, J. Mater. Chem. C 3 (2014) 2016–2023.
[40] R. Duan, C. Li, S. Liu, et al., Determination of adenine based on the fluorescence recovery of the L-ryptophan–Cu^{2+}, complex, Spectrochimica Acta Part A Molecular & Biomolecular Spectroscopy 152 (2016) 272–277.